ISSN No:-2456-2165

# Analysis of Ground Effect Diffuser on a Race Car to Optimize Aerodynamic Performance

ABHISHEK BHARDWAJ
Department of Mechanical Engineering
Kalinga Institute of Industrial Technology, Bhubaneswar
Odisha -751024, India

**Abstract:- Ground effect diffusers have become a prominent aerodynamic device on open-wheeled race cars and sports cars, typically used to generate downforce for better traction. The characteristics and physics that determines downforce generation and its application in automobile and racing industry needs an in-depth analysis to develop a systematic understanding. The amount of downforce generated is dependent of geometrical parameters like ride height, relative length of diffuser to that of the vehicle and the ramp angle. This paper explains the performance of ground effect diffusers and details a numerical investigation of the effects of geometrical parameters in order to find optimum downforce and efficiency for the inverted Ahmed model adapted as a vehicle diffuser bluff body. A short and long diffuser with relative lengths of 0.1 and 0.35 are studied. The short diffuser produced less maximum downforce and efficiency compared to the longer diffuser. Different diffuser ramp angles were found to correspond to different ride heights to achieve optimum efficiency and downforce.**

***Keywords***:- *Ground-Effect, Aerodynamics, Diffuser, Downforce, Efficiency.*

**NOMENCLATURE**

| | |
|---|---|
| $C_d$ | coefficient of drag |
| $C_l$ | coefficient of lift |
| $C_p$ | coefficient of pressure |
| $\bar{C}_p$ | overall pressure recovery coefficient |
| $\bar{\bar{C}}_{pd}$ | diffuser mean effective pressure coefficient |
| $D$ | aerodynamic drag (N) |
| $h$ | bluff body ride height (m) |
| $H$ | bluff body height (m) |
| $h_0$ | vertical distance between diffuser exit's top and bluff body floor plane (m) |
| $h_1$ | plane-wall diffuser inlet height (m) |
| $h_2$ | plane-wall diffuser outlet height (m) |
| $L$ | aerodynamic lift (N) |
| $l_d$ | diffuser ramp surface length (m) |
| $L_B$ | bluff body length (m) |
| $L_D$ | diffuser length (m) |
| $p$ | static pressure (Pa) |
| $p_\infty$ | atmospheric pressure (Pa) |
| $q_\infty$ | freestream dynamic pressure (Pa) |
| $U_\infty$ | freestream velocity ($ms^{-1}$) |
| W | width of diffuser (m) |
| θ | diffuser ramp/divergence angle (deg) |
| ρ | Air density ($kgm^{-3}$) |

## I. INTRODUCTION

Race car performance is strongly affected by aerodynamics. Vehicle stability and handling are primarily dictated by tyre performance which is considerably related to aerodynamic loads, i.e., optimal loading of the tyres by the control of front and rear downforce which can lead to improved braking performance, increased cornering speed and overall stability as discussed in Marchesin et al., 2017. Drag reduction is also an important factor to reduce power loss. The common aerodynamic tools to alter aerodynamic performance of race cars include bodyworks and underfloor, wings with endplates, splitters and spoilers, appendages like barge boards and vortex generators, and the wheels.

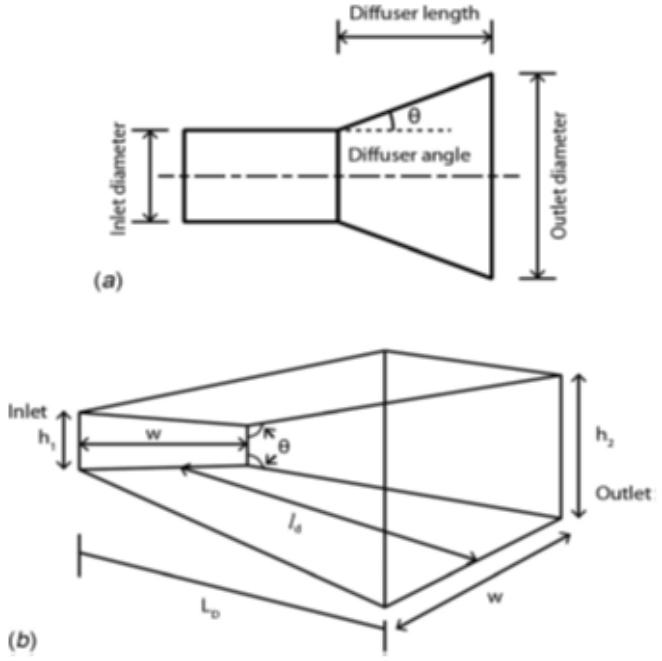


**FIGURE 1.** SCHEMATICS OF (A) 2D CONICAL AND (B) 3D PLANE WALL DIFFUSER (Ehirim et al., 2018)

Bodyworks and particularly the underfloor are the most powerful aerodynamic devices. The diffuser is another similar component in combination with the smooth underbody aft section. Zhang and Zerihan, 2006, shows that ground effect is aimed at producing downforce, via low pressure on the surfaces nearest to the ground. The diffuser also reduces pressure drag, as shown in Bansal and Sharma, 2014, leading to increased aerodynamic efficiency of the vehicle. The aerodynamic phenomenon is attributed to the Bernoulli principle where a static pressure drop occurs

ISSN No:-2456-2165

simultaneously with an increase in velocity of an inviscid fluid.

The basic feature of a diffuser is its increase in cross sectional area from the diffuser inlet to outlet. However, an increase in pressure occurs between inlet and exit, if there is a significant loss in the kinetic energy of the flow. Internal flow diffusers have been used in jet engines, air conditioning and industrial turbomachinery applications before being used in the automotive industry. The pressure recovery coefficient reflects the performance of an internal flow diffuser, which varies with inlet and outlet conditions and the diffuser ramp angle. The basic geometry of internal flow diffuser is shown in Fig. 1. The plane wall diffuser's aspect ratio is $W/h_1$ and area ratio is $h_2/h_1$.

Automobile diffusers generally have a diverging ramp surface at the rear of the underbody. The increasing cross sectional area allows the low-pressure underbody flow to recover its pressure, before merging into the local freestream. Vertical side skirts are also used to prevent leakage and interruption of the low-pressure underbody airflow. The underfloor works as a venturi in ground effect which, when clubbed with a rear diffuser massively reduces the pressure under the vehicle.

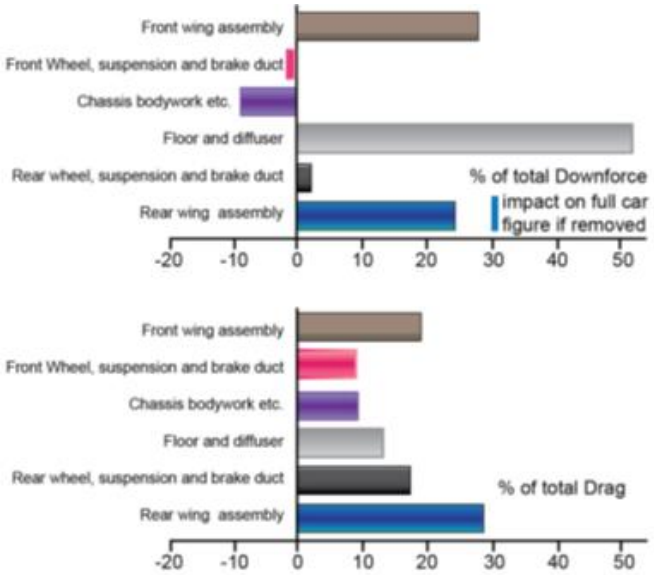


**FIGURE 2.** DOWNFORCE AND DRAG DISTRIBUTION IN AN F1 CAR (Toet, 2013)

This results in downforce generation which enhances traction in track corners by pushing the vehicle's tires onto the ground. This leads to reduced lap times as the car becomes much faster around the corners.

In this paper, we focus on explaining how the ground effect diffuser generates downforce and how its performance is theoretically determined and influenced. We also study the effects of geometrical parameters like ride height, diffuser ramp angle and the relative length for achieving optimum downforce and efficiency, performed in Huminic and Huminic, 2017, and Knight et al., 2018.

## II. DOWNFORCE GENERATION BY GROUND EFFECT DIFFUSERS

There exists an interdependent relationship between aerodynamic drag and downforce. With increase in downforce, which improves traction around on corners, there exists a corresponding increase in drag, which reduces the car's speed on the straights. When compared to the front and rear wings, the underbody with diffuser produces the most downforce with least drag generation, as shown in Fig. 2, discussed in Toet, 2013.

The ground effect diffuser adds downforce by generating a suction effect under the car. The diffuser provides a gradual transition of the high velocity airflow underneath the floor of the car, to the slower exit freestream. The diverging area increases the pressure from the inlet to the outlet of the diffuser. This results in a pressure recovery downstream of the suction peak at the inlet of the diffuser. Thus, the venturi effect and the pressure recovery together generate the downforce. Diffuser ground interaction, diffuser pumping and diffuser upsweep are the three identified downforce mechanisms. Low pressure underneath the car body due to ground effect will generate downforce in any flat-bottomed race car. However, with a diffuser, the underbody pressure can be reduced further. The diffuser provides flow to fixed atmospheric pressure at the outlet. Its pressure recovery controls the pressure under the vehicle. The static pressure recovery is determined by the outlet to inlet ratio of the diffuser, which is dictated by the ramp angle and the ride height. Increased downforce is consequently a result of pump down mechanism which reduces the underbody static pressure, as the airflow proceeds through the diffuser.

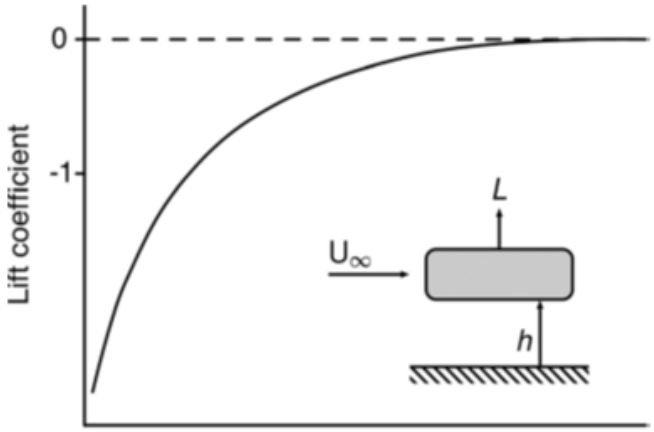


**FIGURE 3.** VARIATION OF NEGATIVE LIFT WITH RIDE HEIGHT OF A SYMMETRICAL BODY (Ehirim et al., 2018)


**FIGURE 4.** INVERTED AHMED BODY ADAPTED AS A DIFFUSER BLUFF BODY

The upward sloping surface of the diffuser ramp describes the diffuser upsweep. The change the flow direction to stick to the ramp requires a resultant pressure force, when it travels through the diffuser. Hence, there is a change in momentum via a change in pressure distribution by a negative camber effect added by the diffuser ramp, which induces additional downforce.

The diffuser and ground interaction explains the association between the ride height and the amount of downforce generated. A symmetrical body without ground effect has zero lift in potential flow. However, a flow asymmetry develops as the height above the ground is reduced.

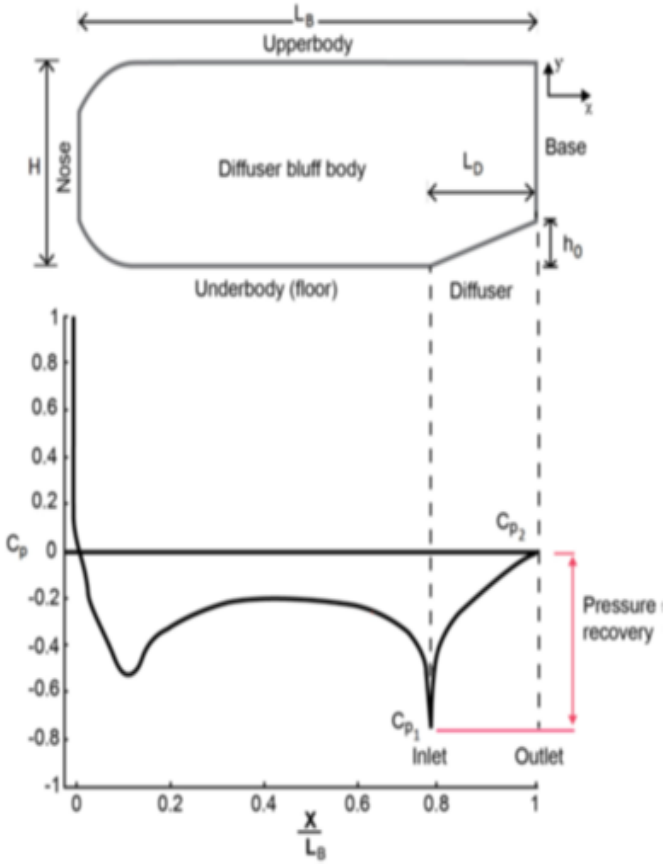


**FIGURE 5.** SCHEMATIC OF CENTERLINE PRESSURE CHARACTERISTIC ALONG THE DIFFUSER BLUFF BODY (Ehirim et al., 2018)

This is due to the accelerated underbody flow in ground effect, resulting in reduction in underbody static pressure. Theoretically, as the ride height reduces to zero, the downforce reaches very large values as shown in Fig. 3. However, in practice, due to blockage effect, the boundary layer developing underside the car limits the maximum achievable downforce. As a result, the downforce reduces with further ride height reduction.

## III. PERFORMANCE OF THE GROUND EFFECT DIFFUSER

The inverted Ahmed body shown in Fig. 4 is a standard geometry which has been adapted in some studies of ground effect diffuser bluff body flows.

The performance of a ground effect diffuser is defined by the static pressure on the surface of the ramp. The pressure coefficient $C_p$ can be used to express the static pressure.

$$C_p = \frac{p - p_\infty}{0.5\rho {U_\infty}^2} \tag{1}$$

The pressure distribution on the diffuser bluff body surface generates a net drag force and downforce on the body. Figure 5 shows the pressure distribution characteristics along an underbody floor.

Assuming that centreline pressures equal average pressures across the bluff body's width $W$ at all cross sections, then aerodynamic lift $L$ and drag $D$ of the body can be shown as

$$L = W\left[\left[\underbrace{\int_0^{L_B-L_D} p_f(x)dx}_{Flat\ Underbody} + \underbrace{\int_{L_B-L_D}^{L_B} p_d(x)dx}_{Diffuser}\right] - \underbrace{\int_0^{L_B} p_u(x)dx}_{Upperbody}\right] \tag{2}$$

$$D = W\left[\underbrace{\int_0^{H} p_n(y)\,dy}_{Nose} - \left[\underbrace{\int_0^{h_0} p_d(y)dy}_{Diffuser} + \underbrace{\int_{h_0}^{H} p_b(y)\,dy}_{Base}\right]\right] \tag{3}$$

Equations (2) and (3) shows the downforce and drag contributions of the diffuser and underbody. The flat underbody, diffuser, upper body, nose, and base of the bluff body are denoted by the subscripts *f,d,u,n,b* respectively.

The performance of a diffuser in an inviscid and incompressible flow was derived in Cooper et al., 2000. The downforce is determined by the difference between the upper body and underbody surface pressures. A simple bluff body was tested with varying underbody geometry and ride heights to investigate the underbody airflow. Over a streamwise length $x_i$, streamwise distance averaged pressure coefficient $\bar{\bar{C}}_{pi}$, was defined as

$$\bar{\bar{C}}_{pi} = \frac{1}{x_i}\int_0^{x_i} C_p(x)dx \quad (3)$$

The specific value of mean effective pressure coefficient along the streamwise length of whole underbody, $\bar{\bar{C}}_{pl}$ is comprised of two components of pressure coefficient: The mean effective pressure coefficient of the flat underbody, $\bar{\bar{C}}_{pf}$, and the diffuser, $\bar{\bar{C}}_{pd}$

$$\bar{\bar{C}}_{pl} = \left(1 - \frac{L_D}{L_B}\right)\bar{\bar{C}}_{pf} + \left(\frac{L_D}{L_B}\right)\bar{\bar{C}}_{pd} \quad (4)$$

The overall pressure recovery coefficient of the diffuser $\bar{C}_p$ was represented using the inlet pressure coefficient, $C_{p1}$, and outlet pressure coefficient, $C_{p2}$

$$\bar{C}_p = \frac{C_{p1} - C_{p2}}{1 - C_{p1}} \quad (5)$$

Considering $p_\infty$ and $q_\infty$, the static and dynamic pressure of the freestream flow, respectively, then the diffuser exit pressure coefficient, $C_{p2}$, is defined as

$$C_{p2} = \frac{p_2 - p_\infty}{q_\infty} \quad (6)$$

The derivation of $\bar{\bar{C}}_{pd}$ was developed in detail in Cooper et al., 2000, and was presented as

$$\bar{\bar{C}}_{pd} = 1 - \frac{(1 - C_{p2})}{\sqrt{1 - \bar{C}_p}} \quad (7)$$

The centreline pressure distribution of the diffuser is non-linear. However, the downforce production of the whole underbody is dictated by the diffuser pressure recovery performance. Thus, for a greater downforce, $\bar{\bar{C}}_{pl}$ needs to be more negative which is a result of $\bar{\bar{C}}_{pd}$ being more negative.

## IV. VALIDATION OF FLOW AROUND DIFFUSER BLUFF BODY

Knight et al., 2018, used an open jet wind tunnel for obtaining pressure distribution along the slanted surface of the inverted Ahmed body centreline. Scani-valves connected to a digital manometer were used to obtain pressure measurements. Inlet boundary conditions for CFD approach were set according to the tunnel cross section of 480 mm, wind speed of 20 m/s and turbulence intensity measured at 1%. The Ahmed body resulted in a blockage ratio of 4% and thus no correction factors were applied since the blockage was less than 5%.

The CFD approach in used a velocity inlet and pressure outlet boundary conditions. Ahmed body surface was set as non-slip wall and remaining boundaries of the domain were set to slip wall conditions. Star CCM+ and Ansys Fluent were used to solve the Navier-Stokes equations using finite volume method. The CFD simulation was setup to provide a result within 10% of the experimental results. This was done to facilitate increased number of simulations with varying parameters within a limited timeframe. Both the k-ε turbulence model and k-ω Shear Stress Transport (SST) turbulence model were used in validation since both of these two-equation models provide a solution to the Reynolds Averaged Navier Stokes (RANS) with a good degree of accuracy at an accepted computational expense.

The pressure coefficient, $C_p$, obtained by non-dimensional pressure distributions from the k-ω SST, the standard k-ε turbulence models and the wind tunnel measurements are shown in Fig. 6.

Accurate results can be witnessed over most of the lower surface of the Ahmed model. Notable inaccuracies can be seen near the start of the diffuser which can affect the magnitudes of coefficient of lift and drag. However, when working with multiple geometric parameters, the characteristics of the curve obtained is more important than the absolute value. As per the CFD results obtained, the flow is accelerated around the inlet of the diffuser leading to high suction peaks. Due to the sparse location of probes in the experimental measurements, the suction peak was not evident. Experimental values validated the k-ω SST results more accurately. More resolution of the simulation and the experiment would improve the validation. However, for a large number of simulations with varying parameters, more significance is given to identifying the trends, and accepting inaccuracies within 10% between CFD and experimental approach.

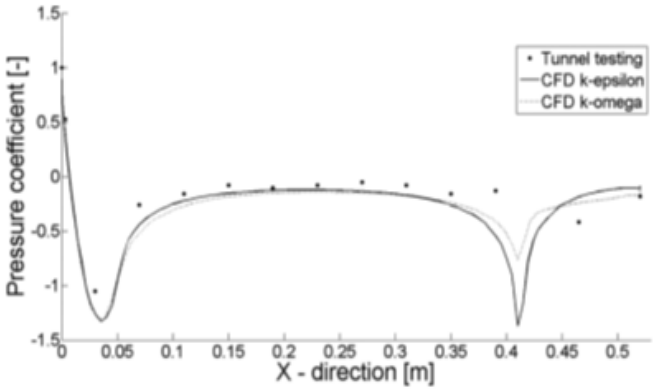


**FIGURE 6.** CENTRELINE PRESSURE DISTRIBUTION OF INVERTED AHMED BODY (Knight et al., 2018)

## V. INVERTED AHMED MODEL IN GROUND EFFECT

Diffuser geometries with relative diffuser lengths of 35% and 10% were investigated in Knight et al., 2018. Diffuser with 35% relative length was referred as the long diffuser and the 10% diffuser relative length as the short diffuser.

Slip wall boundary conditions were applied to the ground to model the moving floor in CFD approach. Polyhedral mesh with mesh base size of 0.13 m was used for the long diffuser. The model minimum and the target mesh

sizes were set to 5% and 10% respectively for a good combination of accuracy and computing time. However, the mesh had to be refined to achieve convergence and generate sensible values, for low ride height, leading to longer computing period. Ramp angles of 5º, 10º, 15º, 20º, 25º, 30º and 35º were investigated for the long diffuser. A maximum angle of 38.5º resulted in a sharp trailing edge for the long diffuser. Ride heights of 5,10,20,30,40 and 50 mm were chosen. A total of 42 simulation runs were performed for all the combinations.

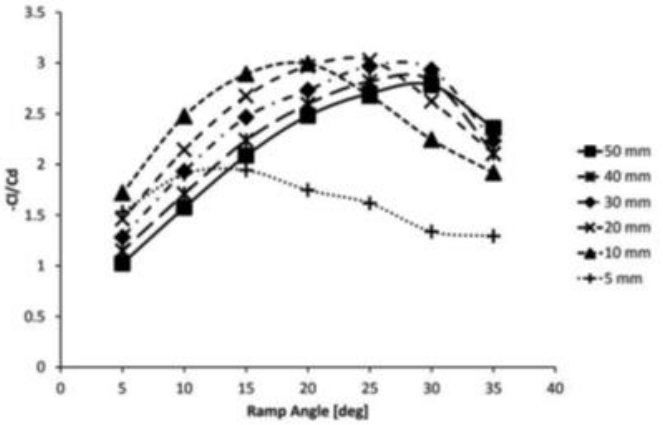


**FIGURE 7.** LINE PLOT OF DOWNFORCE AGAINST RIDE HEIGHT FOR VARIOUS RAMP ANGLES OF LONG DIFFUSER (Knight et al., 2018)

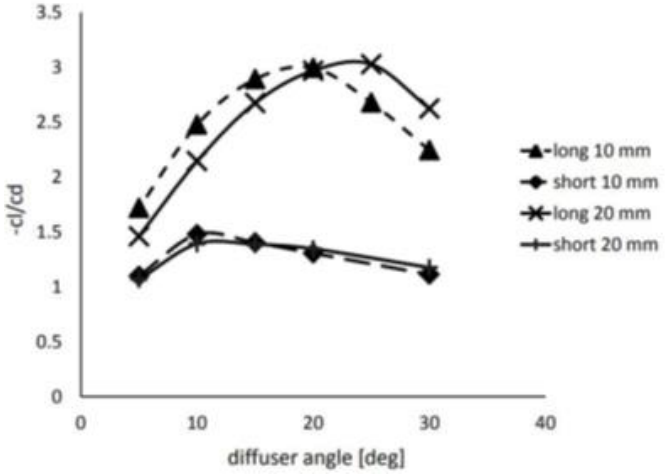


**FIGURE 8.** LINE PLOT OF EFFIENCY RATIO AGAINST RAMP ANGLE FOR VARIOUS RAMP ANGLES OF LONG DIFFUSER (Knight et al., 2018)

Similar combinations were used for the short diffuser as well with changes in meshing. Default tetrahedrons with refining and inflation on the walls was set up for meshing. The Ansys Response Surface Optimization tool was used to find the optimum values using a different analytical approach. Diffuser ramp angle and ride height were fed as inputs in the Design Modeller. Number of mesh elements and mesh skewness for validation of solution and coefficient of lift and drag for optimization were monitored as output parameters. A response surface was created to determine the probability of occurrence of desired solutions. The optimization has been undertaken for maximizing downforce coefficient, $-C_l$, and downforce efficiency, $-C_l/C_d$. Creation of additional simulation points for a new response surface was done once the results from optimization were verified. Convergence was obtained in this closed loop procedure.

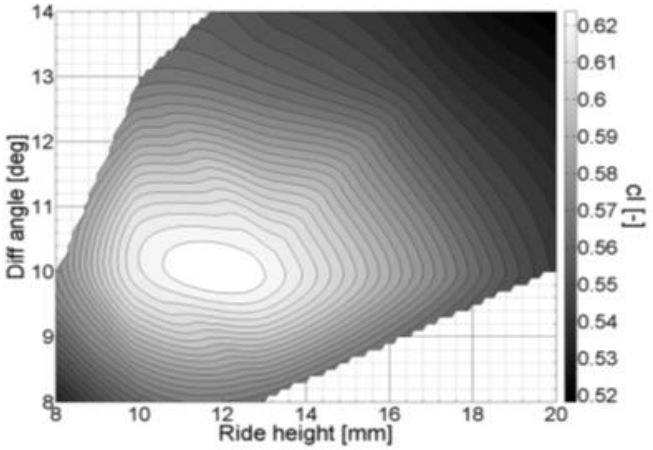


**FIGURE 9.** COUNTER PLOTS OF DOWNFORCE AND EFFICIENCY OPTIMIZATION OF SHORT DIFFUSER (Knight et al., 2018)

## VI. RESULTS

The change in downforce, $-C_l$, for various ride heights and ramp angles of the long diffuser is shown in Fig. 7. The long diffuser experiences an increase in downforce for almost all ramp angles, as the ride height decreases. The 35º diffuser demonstrates a very little change with varying ride heights above 10 mm. A reduction in downforce is seen for all ramp angles, at the minimum ride height. The maximum downforce coefficient of 1.43 was obtained for 20 mm ride height at 25º ramp angle. For a lower ride height of 10mm, the maximum downforce coefficient obtained was 1.41 at 20º ramp angle. The 10º and 5º diffuser ramp angle generated least downforce overall. At 10 mm ride height, the 10º diffuser is closest to optimum whereas the 30º diffuser does not work efficiently due to being too close to the ground. The 35º diffuser is inefficient at all ride heights. At the minimum ride height of 5 mm, none of the diffusers work efficiently.

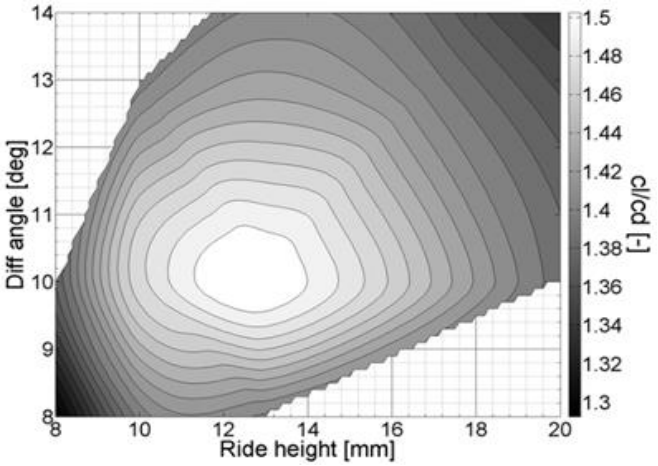


**FIGURE 10.** LINE PLOT OF DOWNFORCE EFFICIENCY FOR LONG AND SHORT DIFFUSERS AT 10 MM AND 20 MM RIDE HEIGHTS (Knight et al.,2018)

The 10mm ride height was optimum for 20º and 10º ramps angles. 25º ramp angle was optimum with 20 mm ride height, and 35º ramp angle for 30 mm ground clearance. We can clearly see that the downforce is a combined function of ramp angle and ride height.

Figure 8 shows that for all ground clearances investigated, there exists a corresponding diffuser angle with highest efficiency. For the long diffuser, the most efficient setup with $-C_l/C_d$ = 3.03, is at 20mm ground clearance with a 25º ramp angle. Here the ground clearance is 3.8% of the length of the model.

Figure 9 shows the results from the optimisation study of the short diffuser. The contour plot of relation of the diffuser's geometrical parameters on the efficiency and downforce are presented. The optimum diffuser ramp angle and the ride height has been found to be 10º and 12mm, respectively, which corresponds to a maximum coefficient of downforce of 0.625. The most aerodynamically efficient ride height ratio was found to be 2.5% of the length of the model, which corresponds to 13 mm ground clearance at the same ramp angle of 10º. This implies that the drag generated has less impact on the efficiency with respect to downforce in short diffusers.

The downforce efficiencies for both short and long diffusers is depicted in Fig. 10 for varying diffuser angles at 10 mm and 20 mm ground clearance. A direct comparison can be made between long and short diffusers, since thee ride heights are in the region of optimal aerodynamic efficiency. The downforce efficiency follows a similar trend for both long and short diffusers with varying ramp angle and ride height. Due to increased surface area, it is noted that the long diffuser has a much higher downforce efficiency compared to the short diffuser. The long diffusers achieve optimal efficiency at higher ramp angles. The sensitivity for short diffusers is lower, which is evident by the profile of efficiencies for the short diffuser.

## VII. CONCLUSION

- The importance of the downforce generated and comparatively low drag of the ground effect diffuser, in comparison to the other aerodynamic components, have been highlighted.
- The aerodynamic mechanisms contributing to the performance of an automotive diffuser have been recognised as diffuser upsweep, diffuser ground interaction and diffuser pumping. These mechanisms allow the ground effect diffuser to act as a pressure recovery device at a much higher divergence angle.
- Downforce values and aerodynamic efficiency were obtained for varying ride heights with multiple ramp angles for a short and a long diffuser.
- For a given ramp angle, downforce increases as the ride height decreases upto a critical value, for maximum downforce generation, beyond which the downforce begins to decrease.
- For a given ride height, downforce increases with increasing ramp angle, upto a limit.
- Downforce can also be increased by increasing diffuser relative length or area ratio. Over a limited range of diffuser ramp angles, an equal maximum downforce can be achieved with larger diffuser angles at higher ground clearances.

## ACKNOWLEDGEMENT

I would like to thank our course instructor, Prof. Swarup Nayak for guiding us to explore various research journals and providing us the opportunity to present this term paper. I would also like to acknowledge the use of Kalinga Institute Of Industrial technology, Bhubaneswar, Digital Library for the ease of access to various research papers.

## REFERENCES

[1]. Bansal, R. and Sharma, R. B., 2014, "Drag reduction of passenger car using add-on devices," Journal of Aerodynamics, 2014, 1–13.
[2]. Cooper, K., R., Sovran, G., and Syms, J., 2000, "Selecting Automotive Diffusers to Maximise Underbody Downforce," SAE Paper No. 2000–01–0354.
[3]. Ehirim, O. H., Knowles, K. and Saddington, A. J., 2018, "A Review of Ground-Effect Diffuser Aerodynamics," Journal of Fluids Engineering, Vol. 141
[4]. Huminic, A. and Huminic, G., 2017, "Aerodynamic study of generic car model with wheels and underbody diffuser," International Journal of Automotive Technology, Vol. 18, No. 3
[5]. Knight, J., Spicak, M., Kuzenko, A., Haritos, G. and Ren, G., 2018, "Investigation of vehicle ride height and diffuser ramp angle on downforce and efficiency," Journal of Automobile Engineering
[6]. Marchesin, F. P., Barbosa, R. S., Gadola, M. and Chindamo, D., 2017, "High downforce race car vertical dynamics: aerodynamic index," Vehicle System Dynamics
[7]. Toet, W., 2013, "Aerodynamics and Aerodynamic Research in Formula 1," The Aeronautical Journal, Vol. 117, Issue 1187, pp. 1–25.
[8]. Zhang, X. and Zerihan, W. T. J., 2006, "Ground Effect Aerodynamics of Race Cars," Applied Mechanics Reviews, Vol. 59, Issue 1